Ecotoxicology and Environmental Safety 259 (2023) 115051

Contents lists available at ScienceDirect

Ecotoxicology and Environmental Safety

journal homepage: www.elsevier.com/locate/ecoenv

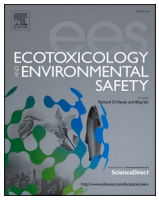

Humic acids alleviate aflatoxin B1-induced hepatic injury by reprogramming gut microbiota and absorbing toxin

Pengfei Xu [a], Shenghui Dong [a], Xinyuan Luo [a], Bin Wei [b], Cong Zhang [b], Xinyao Ji [a], Jing Zhang [a], Xiaoling Zhu [c], Guangfan Meng [a,*], Baolei Jia [d,*], Jie Zhang [a,*]

[a] School of Bioengineering, State Key Laboratory of Biobased Material and Green Papermaking, Qilu University of Technology (Shandong Academy of Sciences), Jinan, China
[b] Shandong Asia-Pacific Haihua Biotechnology Co., Ltd, Jinan, China
[c] Shandong Academy of Agricultural Sciences, Jinan, China
[d] Insitute of Biomanufacturing, Xianghu Laboratory, Hangzhou, China

ARTICLE INFO

Edited by Dr Yong Liang

Keywords:
Humic substance
AFB1
Intestine
Liver
Gut barrier functions
Mice

ABSTRACT

Aflatoxin B1 (AFB1) is a hepatotoxic fungal metabolite that is widely present in food and can cause liver cancer. As a potential detoxifier, naturally occurring humic acids (HAs) may be able to reduce inflammation and restructure the gut microbiota composition; however, little is known about the mechanism of HAs detoxification as applied to liver cells. In this study, HAs treatment alleviated AFB1-induced liver cell swelling and the infiltration of inflammatory cells. HAs treatment also reinstated various enzyme levels in the liver disturbed by AFB1 and substantially alleviated AFB1-caused oxidative stress and inflammatory responses by enhancing immune functions in mice. Moreover, HAs increased the length of the small intestinal and villus height to restore intestinal permeability, which is impaired by AFB1. In addition, HAs reconstructed the gut microbiota, increasing the relative abundance of *Desulfovibrio*, *Odoribacter*, and *Alistipes*. *In vitro* and in vivo assays demonstrated that HAs could efficiently remove AFB1 by absorbing the toxin. Therefore, HAs treatment can ameliorate AFB1-induced hepatic injury by enhancing gut barrier function, regulating gut microbiota, and adsorbing toxin.

1. Introduction

Aflatoxins are carcinogenic noxious substances produced by mold fungi (primarily *Aspergillus flavus* and *Aspergillus parasiticus*) which contaminate stored foods and cereals (El-Shafea et al., 2014; Liu et al., 2022; Romero-Sánchez et al., 2022). Common aflatoxins produced by *Aspergillus* species include aflatoxin B1 (AFB1), AFB2, AFG1, and AFG2. Of these, ABF1 is the most mutagenic toxin and has been recognized as a category 1 A carcinogen in humans by the International Agency for Research on Cancer (Claeys et al., 2020). AFB1 comprises a coumarin nucleus fused with a bifuran ring and pentenone ring (Fig. 1a). AFB1 contaminates various foods, including corn, peanuts, oilseeds, and wheat (Hamza et al., 2022). Crop contamination by AFB1 can negatively impact human and animal health, as well as farmers' income and overall international trade (Chen et al., 2019). In animals, AFB1 leads to decreased growth performance, malnutrition, immunosuppression, liver disease, reproductive dysfunction, and high mortality (Elwan et al., 2022; Monson et al., 2015). Therefore, identifying materials and chemicals that can detoxify AFB1 is crucial.

In natural conditions, humic acids (HAs) are formed from plant and microbial residues through physical and chemical reactions and microbial fermentation (Sarlaki et al., 2019). HAs contain carboxyl, carbonyl, and phenolic hydroxyl groups with large surface areas and porous sponge-like structures (Fig. 1b) (Cao et al., 2022; Xu et al., 2020). The chemical properties of HAs include adsorption, ion exchange, aggregation, and complexation. These properties determine the ability of HAs to adsorb both organic and heavy metal pollutants. Additionally, HAs are robust photodegraders of organic pollutants (Chen et al., 2022; Xu et al., 2022b; Zhang et al., 2022). HAs provide molecules with antibacterial, anti-inflammatory, antioxidant, and immunomodulatory functions (Hammoud et al., 2019; Mudroňová et al., 2020). In traditional medicine, HAs have been used to treat various diseases, including diarrhea, gastritis, gastric ulcers, and colitis (Rusliandi et al., 2020).

Previous studies have revealed that HAs can detoxify AFB1 in broilers (Hamza et al., 2022; van Rensburg et al., 2006). However, the detailed mechanisms of HAs functions remain unknown. In this study,

* Corresponding authors.
E-mail addresses: mengguangfan@qlu.edu.cn (G. Meng), baoleijia@cau.ac.kr (B. Jia), zhangjie@qlu.edu.cn (J. Zhang).

https://doi.org/10.1016/j.ecoenv.2023.115051
Received 9 February 2023; Received in revised form 14 May 2023; Accepted 19 May 2023
Available online 23 May 2023

we explored the detoxification effects of HAs on AFB1. In mice, HAs reduced the toxicity of AFB1, thereby preventing liver injury, and prevented AFB1 from impacting gut microbiota and the intestinal barrier. We suggest that the underlying mechanism for these effects is the absorption of aflatoxin molecules by HAs.

2. Materials and methods

2.1. Mice management

Healthy Kunming mice were obtained from Pengyue Laboratory Animal Breeding Co., Ltd. (Jinan, China; experimental animal use license: SCXK (Lu) 20140007). All animal experiments followed the protocols approved by the Animal Care and Use Committee of the Qilu University of Technology (Shandong Academy of Sciences) (approval number: SWS20190610).

After 5 days of adaptive feeding, ninety Kunming mice (5-weeks-old with a body weight of 28 ± 2 g) were randomly divided into three groups (n = 30). Each group contained half males and half females (15 of each sex). One group was fed a normal diet (Table S1) and used as the control group (named CTRL). The second group was fed a diet with AFB1 (0.75 mg/kg) added (named AFB). For this, the mice food was crushed, and AFB1 powder was added in proportion and stirred well before granulation again. The third group was fed a diet of AFB1 (0.75 mg/kg) (prepared in the same manner as above) and provided with HAs in their drinking water (0.4%, m/v) (named AFB+HAs) (Fig. 1c). Kunming mice typically have a daily food intake of 3–8 g and daily water intake of 4–8 mL. The treatment lasted 54 days, following which all mice were euthanized by cervical dislocation, and the body weight was recorded (Table S2). Liver and intestinal tissues from each mouse were collected for histopathological and statistical analysis. Blood samples, colon tissues, and cecal contents from ten mice were collected and pooled to form a single composite sample for further analysis.

2.2. Histopathological and hematological analysis

Liver and intestinal tissues were fixed in 4% paraformaldehyde overnight before embedding in paraffin. After staining with hematoxylin and eosin (H&E), the morphology of the tissues was examined via light microscopy (AX-300, Jinan Qiangsheng Optoelectronic Instrument Co., Ltd, Jinan, China). The villus length was measured using ImageJ software (Schneider et al., 2012). Blood samples were stored at 25 °C for 20 min and then at 4 °C for 1 h. To obtain the serum, the samples were then centrifuged at 200 × *g* for 15 min at 4 °C. Enzyme-linked immunosorbent assay (ELISA) kits (Nanjing Jiancheng Bioengineering Institute, Nanjing, China) were used to measure antioxidant parameters, including superoxide dismutase (SOD), glutathione peroxidase (GSH-PX), and malondialdehyde (MDA), immune-related factors including IL-6, IL-1β, and TNF-α, and inflammation-related factors, including IgA and IgM, as well as serum total protein (TP), alkaline phosphatase (ALP), alanine aminotransferase (ALT), and aspartate aminotransferase (AST).

2.3. Gene expression level analysis

RNAsio Plus (Takara, China) was used to extract total RNA from the

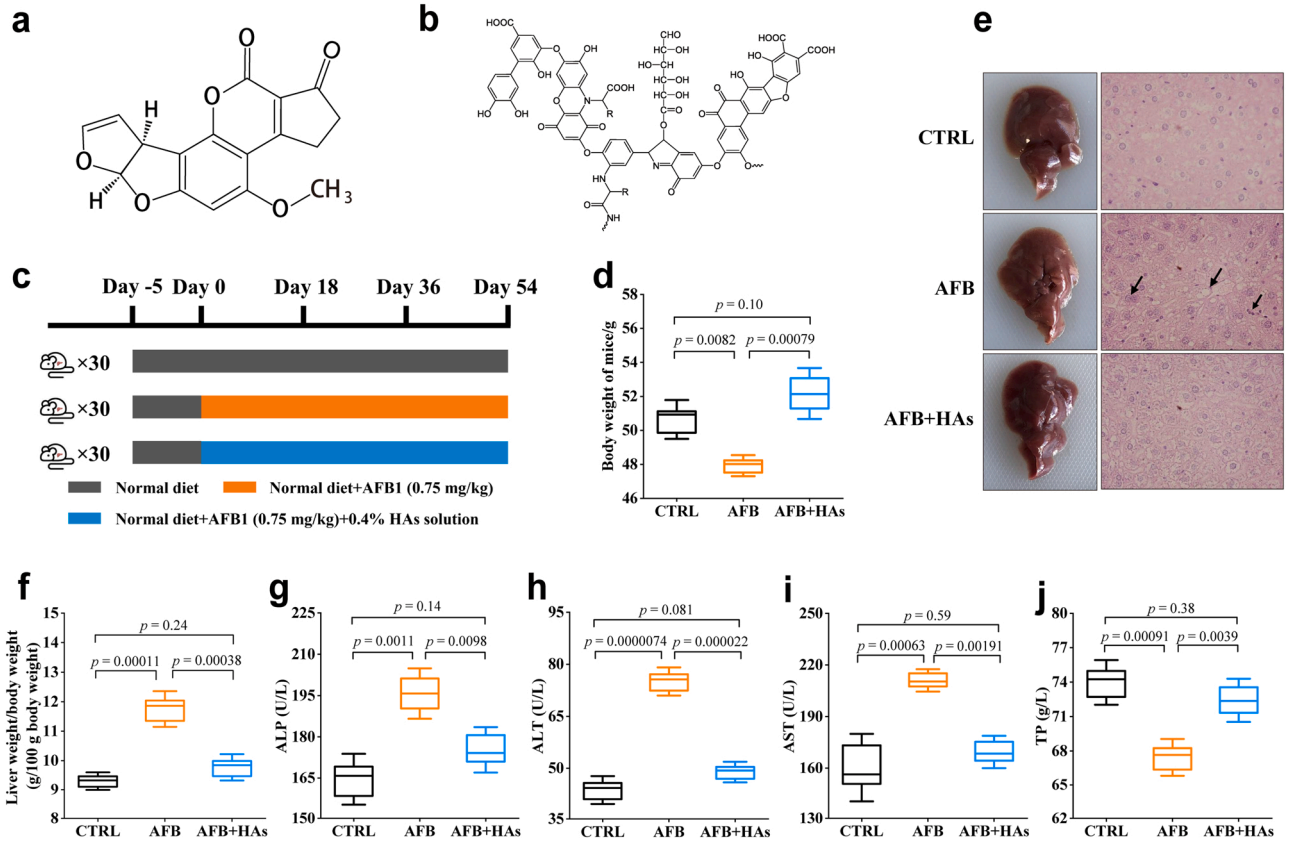

Fig. 1. HAs reduce hepatic injury caused by AFB1 in mice. (a) Chemical structure of AFB1; (b) Chemical structure of HAs; (c) Experimental design of the three mouse cohorts (n = 30 × 3). The three cohorts included a control diet (CTRL), a diet containing AFB1 (AFB), and a diet containing AFB and HAs (AFB+HAs). (d) Variations in body weight at experimental day 1 and day 54 for each group (n = 30). (e) Representative macroscopic liver images and H&E-stained liver sections of each group. (f) Comparison of the ratio of liver weight/body weight (g/100 g) of each group (n = 30). (g–j) Comparison of the levels of alanine aminotransferase (ALT), aspartate aminotransferase (AST), alkaline phosphatase (ALP), and total protein (TP) in the mice sera of each group (n = 30). Significance was determined using the Bonferroni test.

colon tissues according to the manufacturer's instructions. SYBR® Premix Ex Taq™ (Takara, China) was used for Quantitative Real-time PCR (qPCR) following the manufacturer's instructions. GAPDH was used as the internal reference. The primers used for ZO-1, occludin, and claudin-1 were listed in Table S3.

2.4. Analysis of intestinal microbiota

The microbial genomic DNA was extracted from the mice cecal contents using the QIAamp DNA stool kit (QIAGEN, USA). A NanoDrop ND-1000 Spectrophotometer (Thermo Fisher Scientific, USA) was used to quantify the DNA, and the quality was estimated via 1.2% agarose gel electrophoresis. The V3–V4 region of the 16 S rDNA gene was amplified by PCR using forward primer 338 F and reverse primer 806 R (Table S3). For multiplex sequencing, sample-specific 7 bp barcodes were attached to the primers. The amplicons were subjected to 2% agarose gel electrophoresis, and the target fragments were extracted using an Axygen gel recovery kit (SelectScience, UK) and quantified on a microplate reader (BioTek, USA). Sequencing was performed by PersonalBio (Shanghai, China) using the Illumina MiSeq platform (Illumina, USA). Sequence preprocessing and quality control were performed by paired-end ligation and chimera removal. The 16 S sequencing data were processed using QIIME2 2019.4 (Bolyen et al., 2019). The data were deposited in NCBI with the accession number SUB12100692.

2.5. Preparation of mold-contaminated food

The food was fermented at 25 °C with 20% humidity for 1 week in aerobic conditions. The surface of the food was then covered with white and yellow mycelia, and the mycotoxin content in the moldy food was determined using ELISA.

2.6. In vitro adsorption of AFB1 by HAs

Crushed natural mildew corn was passed through a 40-mesh sieve, and the appropriate amount of double-distilled water was added to prepare a 100 ng/mL AFB1 solution. Solid HAs were then added to the solution, resulting in HAs concentrations ranging from 5 to 20 mg/mL (in 5 mg/mL increments), and agitated for 60 min in a temperature-controlled oscillating water bath at 37 °C and 120 rpm with a pH of 7.0. After the reaction, the solution was centrifuged at 3000 g for 10 min, the supernatant was collected, and the process was repeated three times per treatment. An ELISA kit (Bioxl Diagnostic System, USA) was used to detect AFB1 in the samples according to the manufacturer's instructions. The detoxification rate was calculated using Eq. (1):

$$Y(\%) = \frac{C_0 - C}{C_0} \times 100, \quad (1)$$

where C and C_0 are the AFB1 concentrations before and after the reaction, respectively.

2.7. Statistical analysis

Data were analyzed using Origin 2018 software. All results are presented as the mean ± standard deviation of at least three replicates. Significant values were calculated using one-way analysis of variance (ANOVA) followed by the Bonferroni test. A probability level of $p < 0.05$ was considered significant.

3. Results

3.1. HAs alleviate AFB1-induced hepatic injury in mice

We investigated the effect of AFB1 on mice and examined whether HAs can prevent AFB1 toxicity. After consuming the experimental diet for 54 days, the AFB mice had a significantly lower body weight than the CTRL mice ($p = 0.0082$, Fig. 1d). The AFB+HAs mice had significantly higher body weight than the AFB mice ($p = 0.00079$). However, no significant difference was observed between the body weights of CTRL and AFB+HAs mice ($p \geq 0.05$). The principal target of AFB1 is the liver (Li et al., 2019; Liu et al., 2022; Wang et al., 2022). Therefore, we performed histopathological and biochemical analyses of the mice livers. The histopathological analysis revealed that AFB1 exposure resulted in liver damage, inflammatory cell infiltration, and lipid accumulation. The addition of HAs to the AFB1-infected diet attenuated the morphology of the liver (Fig. 1e). AFB1 resulted in an increase in liver/body weight when compared to that in the CTRL group ($p = 0.00011$). The HAs treatment significantly decreased the liver/-body weight when compared to the mice fed with AFB1 ($p = 0.00038$) (Fig. 1f). Meanwhile, the ratio between the CTRL group and the AFB+HAs group did not show significant difference ($p \geq 0.05$). These findings suggest that HAs may aid in restoring body weight and decreasing the liver-to-body weight ratio resulting from AFB1 exposure.

Biochemical markers of liver function, such as serum levels of ALP, ALT, and AST, are typically utilized to assess liver damage. The HAs treatment significantly ameliorated all parameters (Fig. 1g–i). The serum level of TP is another parameter of liver function, which typically decreases in abnormal conditions. In this study, AFBI+HAs treatment significantly increased TP levels when compared to the AFB1 treatment ($p = 0.0039$) (Fig. 1j). In contrast, no significant differences in the biochemical markers were detected between the CTRL and AFB+HAs groups ($p \geq 0.05$).

3.2. HAs restore the physiological steady state in mice damaged by AFB1

To examine the effect of HAs on the antioxidant system in AFB1-exposed mice, we measured the levels of SOD, GSH-PX, and MDA in the serum of each mice group (Fig. 2a–c). AFB1 exposure significantly decreased the SOD and GSH-PX levels ($p = 0.00089$ and $p = 0.0039$, respectively). In contrast, SOD and GSH-PX levels in the AFB+HAs group was significantly higher than those in the AFB group ($p = 0.00035$ and $p = 0.0060$, respectively). The MDA level typically indicates the level of oxidative stress. The AFB group had a significantly higher level of MDA than the CTRL group ($p = 0.000098$). However, the addition of HAs did not significantly affect MDA ($p = 0.16$). These results suggest that HAs may alleviate AFB1-caused oxidative stress within a certain range.

The concentrations of IgA and IgM in the AFB group were significantly lower than those in the CTRL group ($p = 0.015$ and $p = 0.0018$, respectively). However, the intervention of HAs significantly increased the concentrations of IgA and IgM in the serum of the AFB+HAs mice ($p = 0.019$ and $p = 0.0056$, respectively) (Fig. 2d, e), implying that HAs can reduce the immune functional damage caused by AFB1.

We investigated the levels of inflammation-related factors in the serum (Fig. 2f–h). AFB1 exposure significantly increased the concentration of all three factors in the serum when compared to the CTRL group ($p = 0.000056$, $p = 0.000099$, and $p = 0.00050$, respectively). Conversely, HAs significantly reduced the levels of inflammatory factors in the AFB+HAs mice than in the AFB mice ($p = 0.0012$, $p = 0.00070$, and $p = 0.0017$, respectively). However, no significance difference was observed in the antioxidant factors, immunoglobulins, and inflammation factors between the AFB+HAs group and the CTRL group ($p \geq 0.05$). In summary, HAs supplementation provided beneficial effect by preserving the physiological state damaged by AFB1.

3.3. HAs recover intestinal morphology and integrity of the barrier

The intestinal tract acts as a barrier to prevent harmful substances from passing into other tissues. Therefore, the effects of HAs on the gut morphology of AFB1-exposed mice were examined. The length of the small intestine changed in the AFB1 and AFB1 +HAs groups (Fig. 3a).

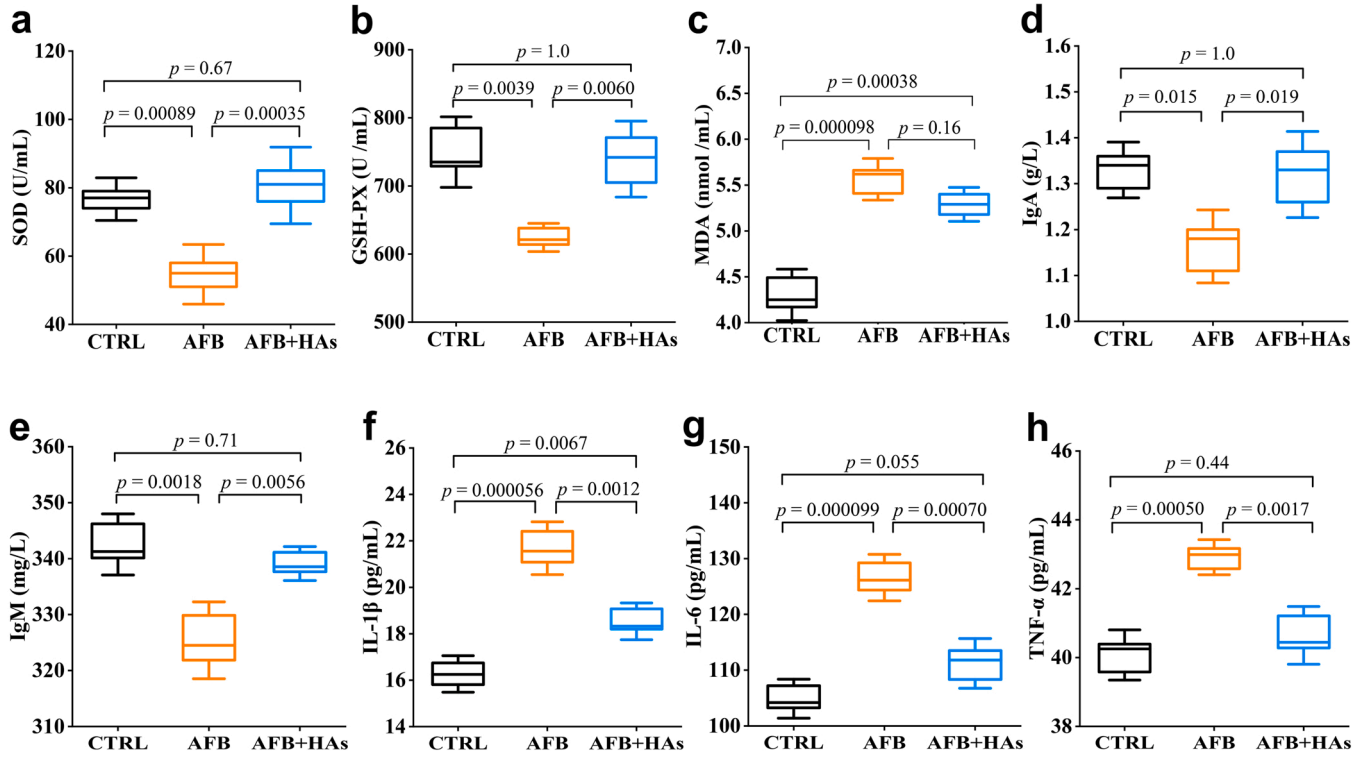

Fig. 2. HAs restore the physiological steady state in mice damaged by AFB1. (a–h) Comparison of the superoxide dismutase (SOD), glutathione peroxidase (GSH-PX), malondialdehyde (MDA), IgA, IgM, IL-1β, IL-6, and TNF-α concentrations in the mice sera of CTRL, AFB, and AFB+HAs groups (n = 30). Significance was determined using the Bonferroni test.

The statistical analysis revealed that the length of the small intestine was significantly shortened in the AFB group ($p = 0.000019$). Conversely, a significant increase in length was observed in the AFB+HAs group than in the AFB group ($p = 0.000064$, Fig. 3b). However, no significant difference was observed in the length of the small intestine between the AFB+HAs group and the CTRL group ($p \geq 0.05$).

The observations of intestinal morphology and H&E staining indicate that AFB1 caused duodenal histological damage (Fig. 3c). However, no significant variation was observed in the duodenal villus height between the AFB group and the CTRL group ($p = 0.67$, Fig. 3d). No significant variation was observed in the duodenal villus height between the AFB+HAs group and the AFB group ($p = 1.0$); however, villus integrity was improved as shown by H&E staining. In contrast, significantly lower villus heights were observed in the jejunum and ileum of the AFB group than in those of the CTRL group ($p = 0.0013$ and $p = 0.000044$, respectively). The AFB+HAs group had significantly higher villus height in the jejunum and ileum than the AFB group ($p = 0.032$ and $p = 0.010$, respectively). The villus height in the jejunum and ileum of the AFB+HAs group was also significantly lower than that of the CTRL group ($p = 0.048$ and $p = 0.00060$, respectively). Finally, compared with the AFB group, the AFB+HAs group alleviated the histological damage caused by AFB1 and significantly increased colonic villus height ($p = 0.026$). The height of the colonic villus also showed no significant difference between the CTRL group and the AFB+HAs group ($p \geq 0.05$). The analysis revealed that HAs can improve intestinal morphology damaged by AFB1 to a certain extent.

We further analyzed the effects of AFB1 and HAs on the expression of the key tight junction proteins (ZO-1, occludin, and claudin-1), which are the biomarkers for the integrity of the intestinal barrier (Zhang et al., 2021). The analysis revealed that AFB1 reduced the expression of genes encoding all three proteins ($p = 0.012$, $p = 0.0032$, and $p = 0.036$, respectively, Fig. 3e). In contrast, the mRNA levels of the three genes were high in the AFB+HAs group ($p = 0.0097$, $p = 0.0011$, and $p = 0.0067$, respectively), suggesting that HAs are beneficial for maintaining the integrity of the intestinal barrier. The findings suggest that HAs have a protective function after the intestinal barrier is damaged by AFB1.

3.4. HAs improve gut microbiota composition in AFB1-treated mice

To analyze whether AFB1 and/or AFB1/HAs treatments alter the gut microbiota in mice, we used 16 S rDNA gene sequencing to determine the composition of the gut microbiota in the mice feces. The operational taxonomic units (OTUs) in the AFB group were lower than those in the CTRL group ($p = 0.011$). Notably, the OTUs in the AFB+HAs group were significantly higher than those in the AFB group and CTRL group ($p = 0.00040$ and $p = 0.021$, Fig. 4a). Venn diagrams revealed the AFB+HAs group contained more specific OTUs than the other two groups (Fig. 4b). The OTU rank curve also showed that the OTU abundance in the AFB+HAs group was highest, followed by the CTRL group and the AFB group (Fig. S1). The α-diversity analysis (including Chao1, Shannon, and Faith's PD) revealed that HAs-treated mice had increased microbial community diversity then the AFB mice and CTRL mice (Fig. 4c–e). Principal component analysis (PCA) revealed that each group clustered separately, suggesting that both treatments (AFB and AFB+HAs) changed the constituents in the gut microbiota (Fig. 4f).

Additionally, we compared the gut microbiota variations at different taxonomic levels. At the phylum level, the HAs group had a significantly decreased relative abundance of Firmicutes ($p = 0.0015$), increased relative abundance of Bacteroidetes ($p = 0.000061$), and thus a declined Firmicutes/Bacteroidetes ratio than the AFB group ($p = 0.00065$) (Fig. 4g–i). Notably, the abundance of Firmicutes was decreased and that of Bacteroidetes was significantly increased in the AFB+HAs group than in the CTRL group ($p = 0.0059$ and $p = 0.000013$, respectively). At the genus level, the AFB+HAs group had significantly decreased relative abundances of *Lactobacillus* and *Clostridia UCG 014* and increased relative abundances of *Desulfovibrio*, *Odoribacter*, *Alistipes*, *Lachnospiraceae NK4A136 group*, and *Eubacterium xylanophilum group* than the AFB group

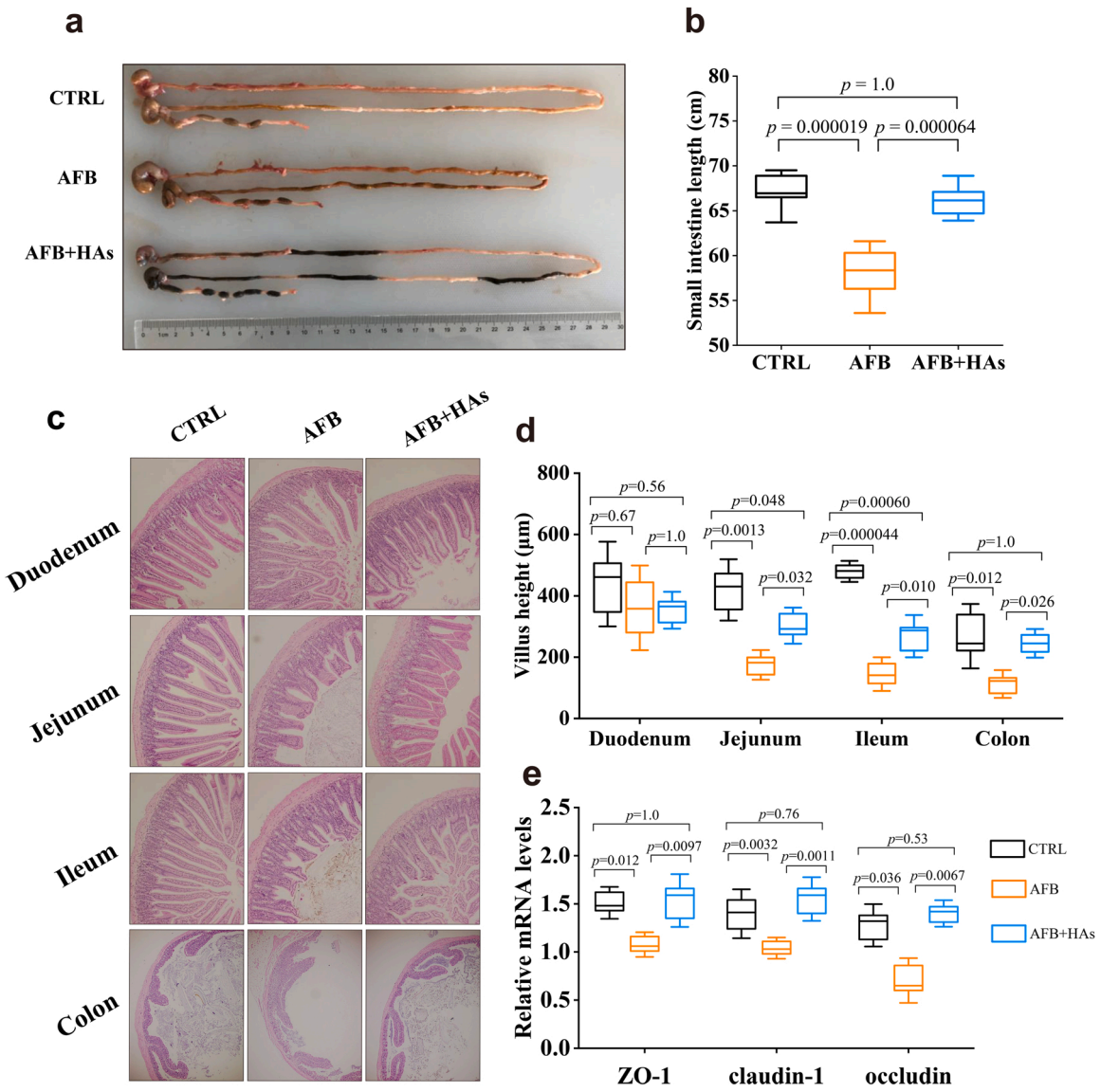

Fig. 3. HAs protect mice from intestinal barrier damage induced by AFB1 exposure. (a, b) Representative photo (a) and statistical analysis of the length (b) of the small intestine in the CTRL, AFB, and AFB+HAs groups (n = 30). (c, d) H&E staining and statistical analysis of the villus height for (b) the duodenum, jejunum, ileum, and colon in each group. (e) Relative expression level of ZO-1, occludin, and claudin-1 in the colon of the three groups (n = 30). Significance was calculated using the Bonferroni test.

(Fig. 4j–o and Fig. S2). Alternatively, significant differences were observed in the abundances of *Lactobacillus*, *Desulfovibrio*, *Odoribacter*, *Alistipes*, and *Eubacterium xylanophilum group* between the CTRL and AFB+HAs groups.

To investigate the different microbiota regulated by AFB1 and HAs, the LEfSe were further analyzed (Fig. S3). At the genus level, the enriched taxa in the AFB group primarily included *Lactobacillus* (LDA = 4.73, $p = 0.027$) and *Clostridia UCG 014* (LDA = 3.70, $p = 0.00$). However, these taxa were not enriched in the AFB+Has group. *Muribaculaceae* (LDA = 4.05, $p = 0.027$), *Desulfovibrio* (LDA = 4.03, $p = 0.039$), and *Odoribacter* (LDA = 3.70, $p = 0.050$) were higher in the AFB+Has group than in the AFB group. This result is consistent with the species composition heatmap (Fig. S4).

3.5. HAs efficiently adsorb AFB1 both in vitro and in vivo

To determine the mechanism involved in HAs detoxification of AFB1 in the liver, we analyzed the AFB1 content in mice feces. Compared with that in feces of CTRL mice, the AFB1 content was higher in the feces of AFB mice. Additionally, AFB1 in the feces of the AFB+HAs group was significantly higher than in the feces of the AFB group ($p = 0.0000065$, Fig. 5a). This result suggests that AFB1 is defecated in the presence of HAs and cannot be absorbed in the intestine. HAs can bind pollutants using the functional groups (Xu et al., 2022b). Therefore, we investigated whether HAs can bind and absorb AFB1. We prepared mold-contaminated foodstuff containing 487.34 ppb AFB1. To investigate the absorption by HAs, the foodstuff with AFB1 was mixed with HAs. The results revealed that AFB1 could be absorbed by HAs at increasing rates with increasing HAs concentrations. In the presence of 15 mg/mL HAs, 90% of the AFB1 was absorbed (Fig. 5b). The results of these assays suggest that HAs can bind AFB1 and prevent AFB1 from entering the circulatory system, thereby decreasing liver toxicity.

4. Discussion

AFB1 is a mycotoxin that is widely present in food and is harmful to both animal and human health. AFB1 exposure can cause chronic hepatic injury (Ghahri et al., 2010; Dai et al., 2022). We revealed that

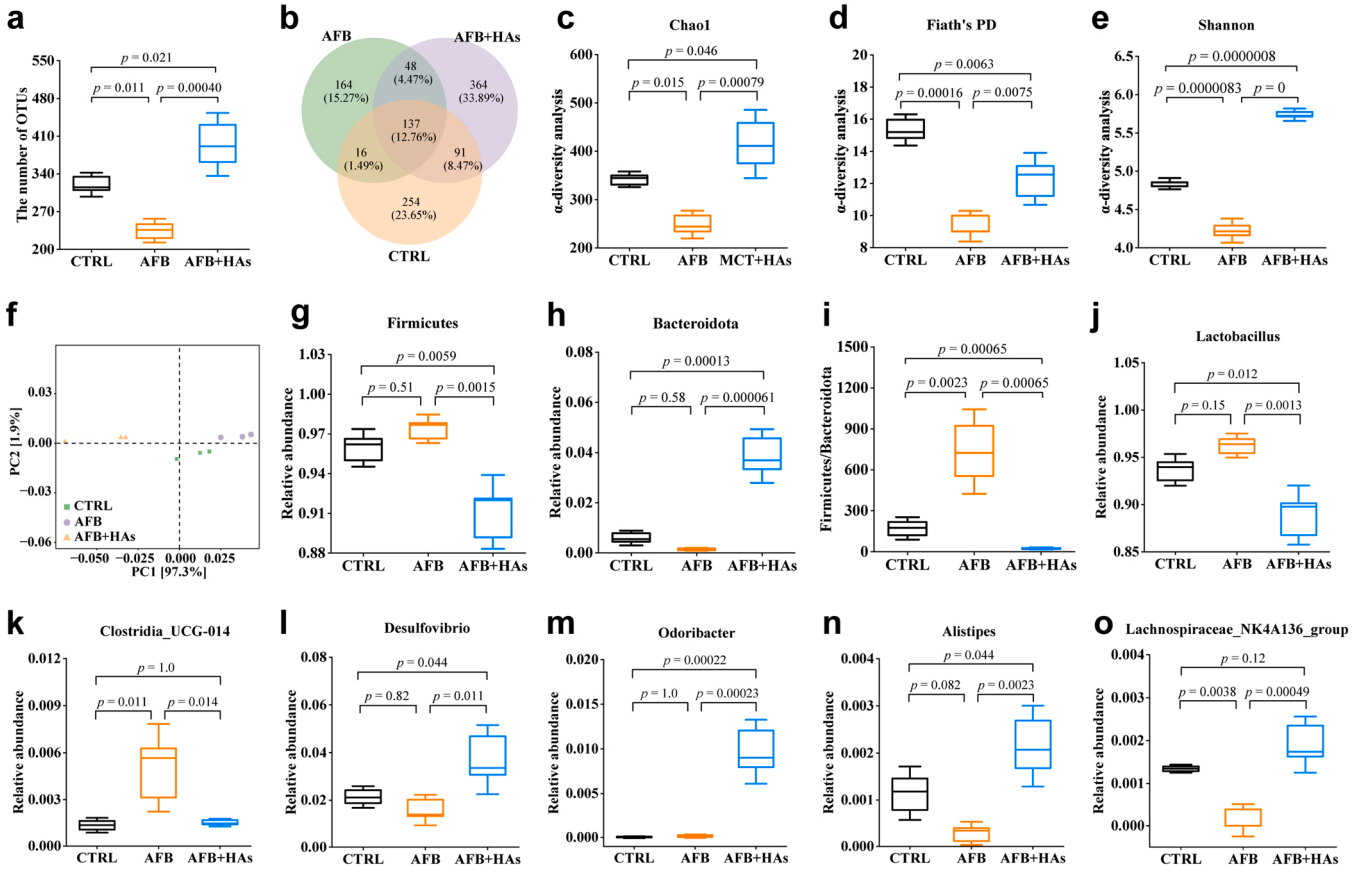

Fig. 4. AFB1 and HAs exposure causes profound changes in the cecal gut microbiota in mice. (a) Number of operational taxonomic units (OTUs) in the gut microbiota of the CTRL, AFB, and AFB+HAs groups. (b) OTU Venn diagram. (c–e) Chao1, Faith's PD, and Shannon indexes of the α-diversity analysis (n = 30). (f) PCA plots showing microbial compositional variation in each group (n = 30). (g–i) Relative abundance of Firmicutes and Bacteroidetes in each group (n = 30). (j–o) Relative abundance of *Lactobacillus*, *Clostridia UCG 014*, *Desulfovibrio*, *Odoribacter*, *Alistipes*, and *Lachnospiraceae NK4A136 group* in each group (n = 30). The unit of relative abundance was calculated based on the percentage of bacterial OTUs identified in the samples. Significance was determined using the Bonferroni test.

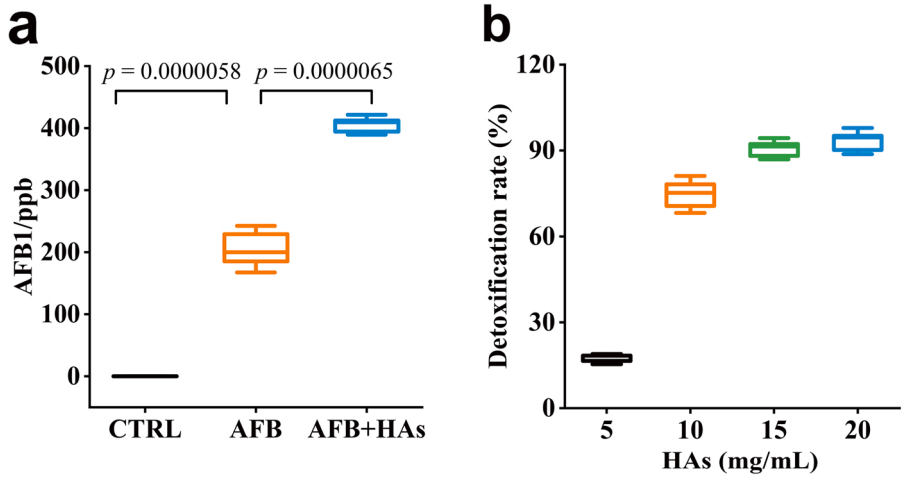

Fig. 5. HAs efficiently adsorb AFB1 in vitro and in vivo. (a) AFB1 content in mouse feces in each group (n = 30). (b) Adsorption efficiency of AFB1 in food at different HAs concentrations (n = 3). Significance was determined using the Bonferroni test.

AFB1 exposure induces lipid accumulation, hepatocyte swelling, and inflammatory cell infiltration. AFB1 also increases the secretion of inflammatory cytokines. HAs attenuated AFB1-induced hepatic injury and oxidative stress and reduced the secretion of pro-inflammatory cytokines in mouse serum. HAs also decreased ALP, ALT, and AST levels and increased TP levels in the mouse serum, which were all impaired by AFB1. The results suggest that HAs can ameliorate AFB1-induced liver injury (Fig. 6).

The intestinal barrier is key to blocking toxic substances and maintaining normal intestinal homeostasis. Several studies have revealed that liver damage caused by AFB1 is associated with a disruption of the gut barrier function (Wang et al., 2019). In the present study, HAs

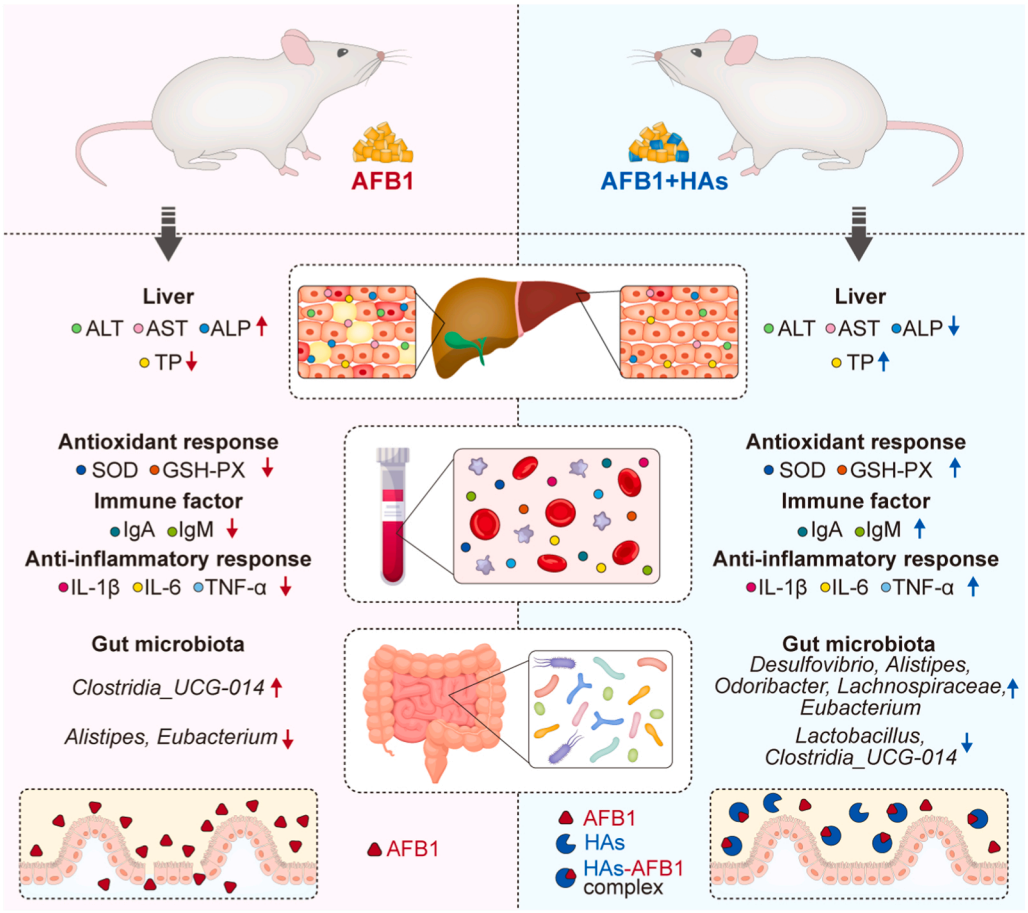

Fig. 6. Mechanisms of HAs to ameliorate AFB1-induced liver injury. AFB1 causes liver injury, increases alanine aminotransferase (ALT), aspartate aminotransferase (AST), and alkaline phosphatase (ALP) contents, and decreases the total protein (TP) content. HAs restore the hepatic parameters caused by AFB1 and ameliorate the AFB1-induced reduction in blood antioxidant factors (superoxide dismutase [SOD] and glutathione peroxidase [GSH-PX]), immune factors (IgA and IgM), and pro-inflammatory factors (IL-1β, IL-6, and TNF-α) by adsorbing AFB1, alleviating intestinal barrier dysfunction, and regulating intestinal microbes in mice (Adobe Illustrator CC 2019, http://ai.nbnhj.cn/).

increased intestinal length, improved jejunal and ileal morphology, and decreased intestinal permeability, which were all damaged by AFB1. Therefore, we propose that HAs not only modulate gut barrier function but also prevent the absorption of toxic substances from the gut into the circulatory system.

Gut microbiota comprise a dynamic and complex ecosystem that aids in the functions of food and drug metabolism, immune regulation, and maintenance of the integrity of the intestinal epithelium (Jia et al., 2022; Jia et al., 2020; Lin et al., 2023; Xu et al., 2022a). Previous studies have revealed that HAs have anti-inflammatory and antioxidant effects and ameliorate hepatic lipid metabolism disorders in different animal models (Jaďuttová et al., 2019; van Rensburg, 2015). However, the preventive effects of HAs on gut microbiota in AFB1-exposed mice have remained unclear. Several previous studies revealed that AFB1 exposure induces oxidative stress, inflammation, and obesity by increasing the Firmicutes/Bacteroidetes ratio (Zhang et al., 2021). Our results are consistent with these previous findings, in that HAs alleviated fatty liver disease, inflammation, and oxidative stress by restoring the Firmicutes/Bacteroidetes ratio. Regarding the different microbiota, previous studies have identified *Desulfovibrio* as a common bacterium associated with states of oxidative stress, with SOD and GSH-PX being positively correlated with *Desulfovibrio* (Li et al., 2021; Ma et al., 2019). The *Lachnospiraceae NK4A136 group* exhibits anti-inflammatory properties and promotes the repair of intestinal mucosa (Zhong et al., 2021), while *Alistipes* has been found to be protective against diseases such as colitis and various liver fibroses (Parker et al., 2020). *Clostridia UCG 014* is a probiotic strain associated with tryptophan metabolism (Yang et al., 2021), and *Odoribacter* has a significant protective effect against colitis and colon cancer in mice (Xing et al., 2021). In this study, HAs prevented the AFB1-induced reduction of *Desulfovibrio*, *Lachnospiraceae NK4A136 group*, *Alistipes*, and *Odoribacter*. The results strongly suggest that HAs affect the gut microbiota and can reconstitute AFB1-induced dysbiosis.

HAs can treat multiple types of organic pollutants, including pesticides, fungicides, antibiotics, and other toxic organic compounds (such as polybrominated diphenyl ethers, nonylphenol, trichloroethane, chloroform, tetrachloroethylene, and polychlorinated biphenyl). The proposed mechanisms used by HAs to treat pollutants include adsorption and photodegradation (Wang et al., 2018; Xu et al., 2019; Xu et al., 2022b). HAs can efficiently adsorb AFB1, both in mice and in vitro. From this study, we propose that macromolecular complexes formed between HAs and AFB1 cannot pass through small intestinal epithelial cells and are excluded from the body, which may be the key mechanism of HAs to treat AFB1 toxicity.

In conclusion, AFB1 exposure leads to liver injury, dysfunction of the intestinal barrier, and alterations in the gut microbiota. Meanwhile, HAs may be a therapeutic approach against AFB1-induced hepatic injury by improving gut barrier function, reconfiguring the gut microbiota, and absorbing toxin. Our study provides evidence that HAs can protect against toxin-induced liver injury by AFB1.

CRediT authorship contribution statement

Pengfei Xu: Methodology, Formal analysis, Investigation, Writing – original draft. **Shenghui Dong**: Investigation, Writing – original draft. **Xinyuan Luo**: Conceptualization, Writing – original draft. **Bin Wei**: Methodology, Sample collection. **Cong Zhang**: Methodology, Sample collection. **Xinyao Ji**: Conceptualization, Sample collection. **Jing Zhang**: Methodology, Software. **Xiaoling Zhu**: Conceptualization, Software. **Guangfan Meng**: Methodology, Investigation, Writing – original draft. **Baolei Jia**: Methodology, Formal analysis, Investigation,

Writing – review & editing. **Jie Zhang**: Funding acquisition, Supervision, Writing – review & editing.

Declaration of Competing Interest

The authors declare that they have no known competing financial interests or personal relationships that could have appeared to influence the work reported in this paper.

Data Availability

The 16S sequencing data of intestinal microbiota are saved in NCBI with the accession number PRJNA884503.

Acknowledgments

This study was funded by the Key Innovation Project of Qilu University of Technology (Shandong Academy of Sciences) [grant number 2022JBZ01-06], National Natural Science Foundation of China (grant number 51978347), Natural Science Foundation of Shandong Province [grant number ZR2021KE038], Shandong Province Agricultural Major Application Technology Innovation Project [grant number 20182130106], and Foundation of Qilu University of Technology of Cultivating Subject for Biology and Biochemistry [grant number 202119]. We would like to thank Editage (www.editage.cn) for English language editing.

Appendix A. Supporting information

Supplementary data associated with this article can be found in the online version at doi:10.1016/j.ecoenv.2023.115051.

References

Bolyen, E., Rideout, J.R., Dillon, M.R., Bokulich, N.A., Abnet, C.C., Al-Ghalith, G.A., et al., 2019. Reproducible, interactive, scalable and extensible microbiome data science using QIIME 2. Nat. Biotechnol. 37 (8), 852–857. https://doi.org/10.1038/s41587-019-0209-9.

Cao, H., Peng, J., Zhou, Z., Yang, Z., Wang, L., Sun, Y., et al., 2022. Investigation of the binding fraction of PFAS in human plasma and underlying mechanisms based on machine learning and molecular dynamics simulation (https://pubs.acs.org/doi/). Environ. Sci. Technol.. https://doi.org/10.1021/acs.est.2c04400.

Chen, B., Xia, Y., He, R., Sang, H., Zhang, W., Li, J., et al., 2022. Water–solid contact electrification causes hydrogen peroxide production from hydroxyl radical recombination in sprayed microdroplets. e2209056119 P. Natl. Acad. Sci. USA 119 (32). https://doi.org/10.1073/pnas.2209056119.

Chen, Y.Y., Lin, Y., Han, P.Y., Jiang, S., Che, L., He, C.Y., et al., 2019. HBx combined with AFB1 triggers hepatic steatosis via COX-2-mediated necrosome formation and mitochondrial dynamics disorder. J. Cell Mol. Med 23 (9), 5920–5933. https://doi.org/10.1111/jcmm.14388.

Claeys, L., Romano, C., De Ruyck, K., Wilson, H., Fervers, B., Korenjak, M., et al., 2020. Mycotoxin exposure and human cancer risk: a systematic review of epidemiological studies. Compr. Rev. Food Sci. Food Saf. 19 (4), 1449–1464. https://doi.org/10.1111/1541-4337.12567.

Dai, H., Liang, S., Shan, D., Zhang, Q., Li, J., Xu, Q., et al., 2022. Efficient and simple simultaneous adsorption removal of multiple aflatoxins from various liquid foods. Food Chem. 380, 132176 https://doi.org/10.1016/j.foodchem.2022.132176.

El-Shafea, Y.M., Hammoud, G.M., Nail, N.S., Salem, A.A., Wahdan, O.A., 2014. In vivo and in vitro evaluation of efficacy of humic acid against aflatoxins. Az. J. Pharm. Sci. 49 (1), 133–154. https://doi.org/10.21608/AJPS.2014.6962.

Elwan, H., Mohamed, A.S., Dawood, D.H., Elnesr, S.S., 2022. Modulatory effects of arctostaphylos uva-urs extract in ovo injected into broiler embryos contaminated by aflatoxin B1. Animals 12 (16), 2042. https://doi.org/10.3390/ani12162042.

Ghahri, H., Habibian, R., Fam, M.A., 2010. Evaluation of the efficacy of esterified glucomannan, sodium bentonite, and humic acid to ameliorate the toxic effects of aflatoxin in broilers. Turk. J. Vet. Anim. Sci. 34 (4), 385–391. https://doi.org/10.3906/vet-0903-19.

Hammoud, G.M., Nail, N.S., Abd El-Shafea, Y.M., Salem, A.A., 2019. Histopathological study on the protective effect of humic acid against aflatoxins induced-oxidative stress in rats. Int. J. Adv. Res. Biol. Sci. 6 (3), 111–127. https://doi.org/10.22192/ijarbs.2019.06.03.007.

Hamza, Z.K., Hathout, A.S., Ostroff, G., Soto, E., Sabry, B.A., El-Hashash, M.A., et al., 2022. Assessment of the protective effect of yeast cell wall beta-glucan encapsulating humic acid nanoparticles as an aflatoxin B1 adsorbent in vivo. e22941 J. Biochem. Mol. Toxicol. 36 (1). https://doi.org/10.1002/jbt.22941.

Jaďuttová, I., Marcinčáková, D., Bartkovský, M., Semjon, B., Harčárová, M., Nagyová, A., et al., 2019. The effect of dietary humic substances on the fattening performance, carcass yield, blood biochemistry parameters and bone mineral profile of broiler chickens. Acta Vet. Brno. 88 (3), 307–313. https://doi.org/10.2754/avb201988030307.

Jia, B., Park, D., Hahn, Y., Jeon, C.O., 2020. Metagenomic analysis of the human microbiome reveals the association between the abundance of gut bile salt hydrolases and host health. Gut Microbes 11 (5), 1300–1313. https://doi.org/10.1080/19490976.2020.1748261.

Jia, B., Han, X., Kim, K.H., Jeon, C.O., 2022. Discovery and mining of enzymes from the human gut microbiome. Trends Biotechnol. 40 (2), 240–254. https://doi.org/10.1016/j.tibtech.2021.06.008.

Li, C., Yan, A., Xie, X., Zhang, J., 2019. Adsorption of Cu(II) on soil humin: batch and spectroscopy studies. Environ. Earth Sci. 78 (15), 1–10. https://doi.org/10.1007/s12665-019-8502-y.

Li, C., Wang, N., Zheng, G., Yang, L., 2021. Oral administration of resveratrol-selenium-peptide nanocomposites alleviates Alzheimer's disease-like pathogenesis by inhibiting abeta aggregation and regulating gut microbiota. ACS Appl. Mater. Interfaces 13 (39), 46406–46420. https://doi.org/10.1021/acsami.1c14818.

Lin, Z., Wu, J., Wang, J., Levesque, C.L., Ma, X., 2023. Dietary Lactobacillus reuteri prevent from inflammation mediated apoptosis of liver via improving intestinal microbiota and bile acid metabolism. Food Chem. 404, 134643 https://doi.org/10.1016/j.foodchem.2022.134643.

Liu, S., Kang, W., Mao, X., Ge, L., Du, H., Li, J., et al., 2022. Melatonin mitigates aflatoxin B1–induced liver injury via modulation of gut microbiota/intestinal FXR/liver TLR4 signaling axis in mice. J. Pineal Res. 73 (2), e12812 https://doi.org/10.1111/jpi.12812.

Ma, H., Zhang, B., Hu, Y., Wang, J., Liu, J., Qin, R., et al., 2019. Correlation analysis of intestinal redox state with the gut microbiota reveals the positive intervention of tea polyphenols on hyperlipidemia in high fat diet fed mice. J. Agric. Food Chem. 67 (26), 7325–7335. https://doi.org/10.1021/acs.jafc.9b02211.

Monson, M., Coulombe, R., Reed, K., 2015. Aflatoxicosis: lessons from toxicity and responses to aflatoxin B1 in poultry. Agriculture 5 (3), 742–777. https://doi.org/10.3390/agriculture5030742.

Mudroňová, D., Karaffová, V., Pešulová, T., Koščová, J., Maruščáková, I.C., Bartkovský, M., et al., 2020. The effect of humic substances on gut microbiota and immune response of broilers. Food Agr. Immunol. 31 (1), 137–149. https://doi.org/10.3390/agriculture11080744.

Parker, B.J., Wearsch, P.A., Veloo, A.C.M., Rodriguez-Palacios, A., 2020. The genus alistipes: gut bacteria with emerging implications to inflammation, cancer, and mental health. Front. Immunol. 11, 906. https://doi.org/10.3389/fimmu.2020.00906.

Romero-Sánchez, I., Ramírez-García, L., Gracia-Lor, E., Madrid-Albarrán, Y., 2022. Simultaneous determination of aflatoxins B1, B2, G1 and G2 in commercial rices using immunoaffinity column clean-up and HPLC-MS/MS. Food Chem. 395, 133611 https://doi.org/10.1016/j.foodchem.2022.133611.

Rusliandi, R., Rousdy, D.W., Mukarlina, M., 2020. The anti-inflammatory activity of humic acid from borneo peat soil in mice. Maj. Obat. Tradis. 25 (1), 22–28. https://doi.org/10.22146/mot.48003.

Sarlaki, E., Sharif Paghaleh, A., Kianmehr, M.H., Asefpour Vakilian, K., 2019. Extraction and purification of humic acids from lignite wastes using alkaline treatment and membrane ultrafiltration. J. Clean. Prod. 235, 712–723. https://doi.org/10.1016/j.jclepro.2019.07.028.

Schneider, C.A., Rasband, W.S., Eliceiri, K.W., 2012. NIH Image to ImageJ: 25 years of image analysis. Nat. Methods 9 (7), 671–675. https://doi.org/10.1038/nmeth.2089.

van Rensburg, C.E., 2015. The antiinflammatory properties of humic substances: a mini review. Phytother. Res. 29 (6), 791–795. https://doi.org/10.1002/ptr.5319.

van Rensburg, C.J., Van Rensburg, C.E.J., Van Ryssen, J.B.J., Casey, N.H., Rottinghaus, G.E., 2006. In vitro and in vivo assessment of humic acid as an aflatoxin binder in broiler chickens. Poult. Sci. 85 (9), 1576–1583. https://doi.org/10.1093/ps/85.9.1576.

Wang, R., Yang, S., Fang, J., Wang, Z., Chen, Y., Zhang, D., et al., 2018. Characterizing the interaction between antibiotics and humic acid by fluorescence quenching method. Int. J. Environ. Res. Public. Health 15 (7), 1458. https://doi.org/10.3390/ijerph15071458.

Wang, W., Zhai, S., Xia, Y., Wang, H., Ruan, D., Zhou, T., et al., 2019. Ochratoxin A induces liver inflammation: involvement of intestinal microbiota. Microbiome 7 (1), 151. https://doi.org/10.1186/s40168-019-0761-z.

Wang, Y., Liu, F., Liu, M., Zhou, X., Wang, M., Cao, K., et al., 2022. Curcumin mitigates aflatoxin B1-induced liver injury via regulating the NLRP3 inflammasome and Nrf2 signaling pathway. Food Chem. Toxicol. 161, 112823 https://doi.org/10.1016/j.fct.2022.112823.

Xing, C., Wang, M., Ajibade, A.A., Tan, P., Fu, C., Chen, L., et al., 2021. Microbiota regulate innate immune signaling and protective immunity against cancer. Cell Host Microbe 29 (6), 959–974. https://doi.org/10.1016/j.chom.2021.03.016.

Xu, B., Lian, Z., Liu, F., Yu, Y., He, Y., Brookes, P.C., et al., 2019. Sorption of pentachlorophenol and phenanthrene by humic acid-coated hematite nanoparticles. Environ. Pollut. 248, 929–937. https://doi.org/10.1016/j.envpol.2019.02.088.

Xu, P., Wang, Y., Li, X., Chen, Q., Hao, L., Zhang, J., et al., 2020. An acidic-groups detection method and its application to analysis of Chinese humic acid samples. PLoS One 15 (8), e0238061. https://doi.org/10.1371/journal.pone.0238061.

Xu, P., Lv, T., Dong, S., Cui, Z., Luo, X., Jia, B., et al., 2022a. Association between intestinal microbiome and inflammatory bowel disease: Insights from bibliometric analysis. Comput. Struct. Biotechnol. J. 20, 1716–1725. https://doi.org/10.1016/j.csbj.2022.04.006.

Xu, P., Zhu, X., Tian, H., Zhao, G., Chi, Y., Jia, B., et al., 2022b. The broad application and mechanism of humic acids for treating environmental pollutants: Insights from bibliometric analysis. J. Clean. Prod. 337, 130510 https://doi.org/10.1016/j.jclepro.2022.130510.

Yang, C., Du, Y., Ren, D., Yang, X., Zhao, Y., 2021. Gut microbiota-dependent catabolites of tryptophan play a predominant role in the protective effects of turmeric polysaccharides against DSS-induced ulcerative colitis. Food Funct. 12 (20), 9793–9807. https://doi.org/10.1039/D1FO01468D.

Zhang, H., Yan, A., Liu, X., Ma, Y., Zhao, F., Wang, M., et al., 2021. Melatonin ameliorates ochratoxin A induced liver inflammation, oxidative stress and mitophagy in mice involving in intestinal microbiota and restoring the intestinal barrier function. J. Hazard. Mater. 407, 124489 https://doi.org/10.1016/j.jhazmat.2020.124489.

Zhang, Y., Yuan, Y., Tan, W., 2022. Influences of humic acid on the release of polybrominated diphenyl ethers from plastic waste in landfills under different environmental conditions. Ecotoxicol. Environ. Saf. 230, 113122 https://doi.org/10.1016/j.ecoenv.2021.113122.

Zhong, Y.B., Kang, Z.P., Wang, M.X., Long, J., Wang, H.Y., Huang, J.Q., et al., 2021. Curcumin ameliorated dextran sulfate sodium-induced colitis via regulating the homeostasis of DCs and Treg and improving the composition of the gut microbiota. J. Funct. Foods 86, 104716. https://doi.org/10.1016/j.jff.2021.104716.